Drug-mediated metabolic tipping between antibiotic resistant states in a mixed-species community

Robert E. Beardmore[1+*], Emily Cook[1+], Susanna Nilsson[1],
Adam R. Smith[3], Anna Tillmann[4], Brooke D. Esquivel[3]
Ken Haynes[1†], Neil A. R. Gow[4], Alistair J. P. Brown[4],
Theodore C. White[3] and Ivana Gudelj[1*]

[1]Biosciences, University of Exeter, Exeter, UK,
[3]School of Biological Sciences, University of Missouri at Kansas City, Kansas City, MO, USA
[4]MRC Centre for Medical Mycology,
University of Aberdeen, Institute of Medical Sciences, Foresterhill, Aberdeen, UK

[+]Authors contributed equally;
[*]To whom correspondence should be addressed;
E-mails: r.e.beardmore@exeter.ac.uk; i.gudelj@exeter.ac.uk
[†] Passed away 19th March 2018

Microbes rarely exist in isolation, rather, they form intricate multi-species communities that colonise our bodies and inserted medical devices. However, the efficacy of antimicrobials is measured in clinical laboratories exclusively using microbial monocultures. Here, to determine how multi-species interactions mediate selection for resistance during antibiotic treatment, particularly following drug withdrawal, we study a laboratory community consisting of two microbial pathogens. Single-species dose responses are a poor predictor of community dynamics during treatment so, to better understand those dynamics, we introduce the concept of a dose-response mosaic, a multi-dimensional map that indicates how species' abundance is affected by changes in abiotic conditions. We study the dose response mosaic of a two-species community possessing a 'Gene×Gene×Environment×Environment' ecological interaction whereby *Candida glabrata*, which is resistant to the antifungal drug fluconazole, competes for survival with *Candida albicans*, which is susceptible to fluconazole. The mosaic

comprises several zones that delineate abiotic conditions where each species dominates. Zones are separated by loci of bifurcations and tipping points that identify what environmental changes can trigger the loss of either species. Observations of the laboratory communities corroborated theory, showing that changes in both antibiotic concentration and nutrient availability can push populations beyond tipping points, thus creating irreversible shifts in community composition from drug sensitive to drug resistant species. This has an important consequence: resistant species can increase in frequency even if an antibiotic is withdrawn because, unwittingly, a tipping point was passed during treatment.

Antimicrobial resistance poses a formidable challenge for medicine with resistance to all but the most recently discovered antibiotics encountered in clinical and agricultural practice (*1*). Seeking behavioural changes in antibiotic prescription to control resistance is a field of active theoretical, laboratory and clinical research. Importantly, it has been mooted that resistance could be eliminated using evolution-aware strategies that reverse the arrow of time (*2*). But is drug resistance reversible? And if not, why not?

Antibiotic cycling, whereby different antibiotics are prioritised and restricted through time, can lead to the reversal of resistance if resistant microbes pay the price for their abilities to resist by having reduced fitness when drugs are not around (*3, 4*). This idea has been tested clinically, with mixed outcomes. Restricting use can reduce resistance (*5,6*) though not always (*7*) and, perversely, increases in resistance have been observed following drug restrictions (*6, 8*). Thus clinical strategies that cycle antibiotics have unpredictable effects: they can work (*9–13*) but sometimes they fail (*14, 15*). It is unclear why a self-evidently worthwhile strategy of antibiotic withdrawal would not reduce resistance. An absence of fitness costs of resistance (*16*) is one potential explanation but, in microbial communities, as we now explain, there is another.

Our explanation is this. For simplicity, imagine a microbial community dominated by two species, S and R. Assume the former is sensitive to an antimicrobial and the latter is resistant. Suppose S can invade, and displace, R in the absence of drug and R can invade and displace S in the presence of drug; in this case the drug resistance phenotype of the community is reversible. However, if, now in a different community, R invades and displaces S in the presence of drug but, in the drug's

absence, the community exhibits a frequency dependent bistability (*17*) whereby either R *or* S can dominate, then this community need not have reversible resistance. Here, application of drug forces R to become dominant and the inability of S to always re-invade following withdrawal could cause resistance not to reverse. Now a tipping point is said to occur when S can no longer invade and we provide theoretical mechanisms and microbial data demonstrating how the irreversibility of resistance can arise through tipping.

Metagenomic analyses are rapidly improving our understanding of microbial communities. We now know that antibiotics affect communities in load (*18*) and in diversity (*19*) and, intriguingly, the removal of antibiotic sometimes (*20, 21*) but not always (*22, 23*) restores the community to its original, pre-treated composition. However, selection for resistance within communities is poorly understood because key pharmacological indicators, like the minimal inhibitory concentration (MIC), dose-responses, between-antibiotic drug interactions and costs of resistance are measured in single-species assays. These assays ignore the antibiotic's true context: while microbes can exist as single-species populations, in bloodstream infections, say, most real-world microbes thrive in communities. Why, therefore, should a single-species understanding of microbial responses to antibiotics completely explain resistance progression on the skin, in the gut or a hospital ward?

To support this view, here we show that single-species resistance measures can be poor predictors of resistance in a synthetic microbial community both during treatment, and after antibiotic withdrawal, because of a hitherto unobserved phenomenon: communities can have tipping points when abiotic parameters like treatment duration, antibiotic dose and nutrient availability vary. For example, clinicians vary dosing regimens (*24–26*) and treatment duration (*27*) of critically ill patients while nutrient availability, in the form of glucose concentration, can vary from $0.01 - 0.28\%$ in urine (*28*) to $0.1 - 2.7\%$ in blood with substantial daily variation (*29, 30*). The impact of this on drug resistance is unknown.

We explore resistance and abiotic variation in the simplest possible community of two species, *Candida albicans* and *Candida glabrata*. Both are commensal microbes found together in the microbiota of healthy individuals but they are also opportunistic pathogens causing mucosal infections (*31*) and life-threatening disseminated infections among immunocompromised patients (*32*). Difficult to diagnose, *Candida* infections are associated with high mortality rates, ranging from 46-75% for *Candidiasis* in the bloodstream (*33–35*). Strikingly, as many people die each year from the top ten

invasive fungal diseases, including candidiasis, as do from tuberculosis or malaria (*33*). Apart from its substantial impact on human health, our community treatment model is suited to studying drug withdrawal dynamics because *C. glabrata* infections are relatively unresponsive to the most frequently used antifungal drug fluconazole, while *C. albicans* is sensitive to fluconazole (*36*). Monoculture dose response assays demonstrate this for our study strains at clinical doses (Supporting Fig. S2).

We determined temporal dynamics of the *Candida* species empirically by monitoring their relative frequencies. For this we co-cultured both in shaken, 96-well plates containing liquid growth media supplemented with glucose and fluconazole. The plates were inoculated with a mixture of fluorescently labelled *C. albicans*, at proportion f, and *C. glabrata*, at proportion $1-f$. After 24h of growth (*a.k.a.* one season) densities and frequencies of each species were determined using flow cytometry and a fixed volume sample (3.3%) of the community was transferred to a new 96-well plate containing fresh media, marking the beginning of a new season (Methods).

Applying single-species logic to this community, the resistant species, *C. glabrata*, should dominate in the presence of enough drug. Indeed, there is evidence this is predictive of clinical outcomes: the use of fluconazole prophylaxis was found to influence the proportion of *C. albicans* and *C. glabrata* isolated from the blood of patients with candidemia (*37*), leading to an increase in *C. glabrata* frequency. Fluconazole withdrawal should then shift the community towards the sensitive species, *C. albicans*. Importantly, we can replicate both these observations using our community: under fluconazole treatment the drug resistant *C. glabrata* dominates and when the drug is removed, the sensitive *C. albicans* subsequently recovers. This creates a repeatable, cyclical dynamic as the drug is repeatedly applied and withdrawn (Figure 1(a)).

But is this the only dynamic possible following fluzonazole withdrawal? To answer this we now systematically explore community dynamics under different abiotic conditions by applying ideas from microbial population biology (*38*). Recalling *C. albicans* are inoculated into the microcosm at proportion f, suppose F denotes the frequency of *C. albicans* after one season, so $R(f) = F/f$ denotes the change in *C. albicans* relative frequency. Now, $F = f \cdot R(f)$ is a 'single-season frequency change map' that gives the frequency of *C. albicans* after one season and we will write F as a mathematical function, calling it Φ, thus $\Phi(f) = f \cdot R(f)$. Repeated applications of Φ to frequency values can therefore be used to determine the *C. albicans* frequency after any number, $n \geq 1$, of seasons, provided a given initial (inoculum) frequency f_0 is known. So, $f_1 = \Phi(f_0)$ is the frequency

of *C. albicans* after one season, $f_2 = \Phi(\Phi(f_0)) = \Phi(f_1)$ is the frequency of *C. albicans* after two seasons, $f_3 = \Phi(\Phi(\Phi(f_0))) = \Phi(f_2)$, and so on. In population dynamics theory it is common to write season number as a subscript n, so $f_{n+1} = \Phi(f_n)$ is a shorthand representation of the season-by-season dynamics at season n. It follows by definition that $\Phi(0) = 0$ because with no *C. albicans* in the inoculum, it cannot appear subsequently. Similarly, $\Phi(1) = 1$ must hold as a closed community containing only *C. glabrata* initially must always do so (see Supplementary Information 2 for details).

What should a biologically reasonable Φ look like? Figure 1(b) shows four lab-derived exemplars and we also use a bottom-up mathematical model that builds theoretical Φ functions (Figure 1(c), Supplementary Information 3). The latter can incorporate many microbial life history traits and environmental variables but here we focus on antimicrobials (at concentration a) and extracellular nutrient concentrations, say g denoting the carbon source glucose. We restrict attention for now to just a, ignoring g dependence, and write $\Phi(f, a)$ to emphasise this.

We now ask how the community responds to an antimicrobial by introducing a sequence of antimicrobial dosages, a_n, so that $f_{n+1} = \Phi(f_n, a_n)$ where the treatment can change with each season. In the clinic, a_n might be one of two extremes, either a high dosage above the drug's MIC (minimal inhibitory concentration) or zero when treatment stops. Figure 1(c) shows two theoretically-constructed Φ functions, Φ_{on} and Φ_{off}, motivated by this clinical context:

$$f_{n+1} = \begin{cases} \Phi_{\text{on}}(f_n) & : \text{ if antimicrobial is applied (so } a_n \geq \text{MIC)}, \\ \Phi_{\text{off}}(f_n) & : \text{ if antimicrobial is not applied (so } a_n = 0). \end{cases}$$

Empirical Φ functions (Figure 1(b)) strongly resemble their theoretical counterparts (Figure 1(c)) and, in these figures, both theory and data exhibit reversible resistance.

However, theory-derived Φ_{on} and Φ_{off} provide information about when not to expect reversible resistance (Figure 2(a-d)) and the shape of these two functions is all-important. If Φ_{on} satisfies $\Phi_{\text{on}}(f) < f$ for all f between 0 and 1, then $f_{n+1} = \Phi_{\text{on}}(f_n) < f_n$ follows, meaning the frequency of *C. albicans* decreases each season when drug is applied (Figure 2(a)). Conversely, if $\Phi_{\text{off}}(f) > f$ for all f then *C. albicans* increases each season after treatment withdrawal, whence resistance is reversible (Figure 2(b)). Points of separation, or separatrixes, between these two cases arise when there are frequencies, f, for which $\Phi_{\text{off}}(f) = f$ (Figure 2(c,d)). As a consequence, for our purposes a tipping point, f_u, satisfies $\Phi_{\text{off}}(f_u) = f_u$ and other technicalities (Supplementary Information 2 and 4) . This condition allows either *C. albicans* or *C. glabrata* to dominate in the absence of drug

and, as a result, drug treatment can coerce the microcosm towards either possibility when treatment stops (Supplementary Information 4).

Using a fixed-glucose stochastic model $f_{n+1} = \Phi(f_n, a_n) + \sigma_n$, where σ_n is small-variance noise and the form of Φ is defined in Supplementary Information 3, we show that resistance need not be reversible because a tipping point is encountered in a theoretical 4-day treatment (Figure 2(f-g)) that is not encountered if treatment terminates at 3 days (Figure 2(e)). Figure 2(h,i) then incorporates glucose dependence, g, and explores a model $\Phi(f, a, g)$ in different abiotic conditions by systematically varying g and antibiotic dose, a (Supplementary Information 3.2 and 4). This is impossible to do in empirical microbial ecologies but computational simulations (Figure 2(h)) show the dominant *Candida* species, *albicans* or *glabrata* or neither, in the (a, g)-plane (this is the 'dose-response mosaic'). This computational analysis shows the dosage at which tipping occurs depends on glucose availability and we will therefore now also manipulate glucose availability in our empirical microcosm.

So does the laboratory treatment community also possess tipping points when antibiotic dose or else glucose availability vary? This is difficult to assess directly for several reasons. First, our modelling framework is general but simple and so is not able to accurately pinpoint tipping points in an empirical context. Second, theoretical tipping mechanisms require an unstable fixed point (f_u) under drug-free conditions. These are hard to identify empirically because observations move away from unstable fixed points and so these points, if present, cannot be detected directly in longitudinal data, we can only infer their presence. Other warning signals of tipping exist (*39, 40*) for example so-called 'critical slowing down' (*41, 42*), slow recovery from perturbations (*43, 44*), an increase in autocorrelation (*45*), an increase in the variation of fluctuations (*46, 47*) or timeseries skewness (*48*). We therefore chose variance increases because modelling indicates between-replicate variance (BRV) should increase sharply at a tipping point (Figure 3).

We sought antibiotic tipping experimentally for three treatments, α, β and γ that are designed to explore the dose response mosaic as fully as possible. First, α) glucose is held constant but the drug steadily withdrawn; β) glucose and drug are held constant and γ) glucose is reduced while the drug is withdrawn (Figure 4(a)). For these treatments, glucose varied between $0.1 - 4\%$ mirroring prior *in vitro Candida* experiments (*49, 50*) and fluconazole varied between $0 - 3\mu$g/ml, mirroring prior *in vitro* drug-adaptation studies (*51*).

Treatments α and β lead to reversible resistance (Figure 4(b)) whereby the *C. albicans* frequencies on the last season have almost unimodally distributed between-replicate variation (BRV) (Figure 4(c)). However, treatment γ exhibits characteristics of tipping: BRV statistics of *C. albicans* frequencies on the last observed season approximate a uniform distribution (Figure 4(c)) and mean BRV spikes on season 6 (approximately $8\times$ increase, Figure 4(d,e)). The rapid divergence of replicate trajectories (Figures 4(b), Supporting Fig. S12) that forms a uniform distribution of treatment outcomes for γ (Figure 4(c)) in a manner consistent with theory (Supporting Fig. S9) means that many community trajectories have not returned to their inoculum positions, in contrast to reversible resistance (Figure 1(a)) where they have.

Discussion

The reversibility of resistance is often conceptualised through resistance costs (*16*), a property which ensures resistance genes are lost following drug withdrawal due to a fitness reduction of the mutants that carry them. However the analogy of resistance costs between species is difficult to define. For example, without the drug in our community the *Candida* species have different metabolism (*52*) from which complex, density and frequency dependent ecological interactions like cheating and cooperation can result (*53*). Indeed, the myriad ecological interactions present in natural communities are necessarily perturbed by an antibiotic drug so a model of resistance progression in which resistant and susceptible microbes differ by a single allele will have limited explanatory power here. Thus we invoke tipping as a new mechanism for understanding the dynamics of drug resistance following exposure to antibiotics.

The explanation behind the tipping-induced irreversibility of resistance is this: if a community could persist in multiple configurations in the absence of drug (*17*), antibiotics, indeed, any abiotic perturbation, might push the community into the 'basin of attraction' of the most resistant configuration from all those available. So even if treatment stops, resistance species' frequencies could increase. Our mathematical models illustrate just two basins of attraction, one above the tipping point and one below (Figure 3(a)) but real-world communities may well have more.

Unfortunately, the key ingredient for tipping, multi-stability, is known to be difficult to demonstrate in real communities (*17*) but if present, we then know the removal of drug can create an uncertain future for that community. Figure 3(b) and 4(b) show in theory and in data how some

of those divergent futures pan out; some return whence they came, others move towards a new configuration of the community. This is the defining property of multistability (*17*) and if this new configuration comprises more species that are less susceptible to the drug than were there prior to treatment, resistance in the community will increase even though treatment has stopped.

Our microcosms highlight just one treatment consistent with this theory (Figure 4) but what other treatments might do this? Indeed, data show that not all drug treatments induce tipping (Figure 4). However, mathematics answers the question: any co-variation of abiotic environment and drug, whether stochastic, cyclical, gradual or abrupt that guides the community into a region of the dose-response mosaic that exhibits multi-stability (Figure 2(h) grey zone) creates the right conditions for tipping. Our empirical data provides one example of this (treatment γ) from the infinitely many treatments we could have tested and the mathematical model we present undergoes tipping with this type of treatment (Supporting Fig. S9) and for many more besides. The theoretical treatment examples we provide (Figure 3 and Supporting Fig. S10) illustrate, perhaps, the simplest possible abiotic variation that can exhibit tipping, namely the abrupt cessation of a constant-dose drug treatment (Figure 3) of the kind given to patients in the community.

To conclude, we argue that single-species logic is insufficient to understand resistance in microbial communities. Particularly lacking is a theory of how abiotic variation promotes resistance and yet this is relevant to patients. For example, infections involving *C. glabrata* are more frequently found in diabetic patients with high blood glucose levels than in patients with lower glucose levels (*54, 55*), indicating that nutrient availability may play a role in clinical resistance, just as it does in our community. Our observations may also indicate potential for alternative therapeutic rationales for polymicrobial infections. Diet is known to alter the host microbiota (*56–58*) and so fashioning specific environments by manipulating nutrients might tip the balance of competition in favour of drug-susceptible species and render an infection more amenable to treatment. There is a precedence for this idea (*59–61*).

Methods

Strains and assay medium

The strains *Candida albicans* ACT1-GFP and *Candida glabrata* ATCC2001 were used throughout this paper in all Experimental designs $1-3$. The strain *C. albicans* ACT1-GFP strain is SBC153 (*62*) with pACT1-FLAG-GFP integrated at the ACT1 locus by means of positive selections using a nourseothricin resistance cassette. The strain *C. glabrata* ATCC2001 is the wild type reference strain obtained from the American Type Culture Collection. The assay medium throughout was synthetic complete (SC) (0.67% w/v yeast nitrogen base without amino acids, 0.079% w/v synthetic complete supplement mixture (Formedium, Hunstanton, UK)).

Measuring growth of *C. albicans* and *C. glabrata* in isolation in the absence / presence of drugs

Overnight cultures in YPD of C. albicans and C. glabrata were diluted, counted on hemocytometer, and adjusted to 2×10^7 cells/mL in SC medium containing 2% (weight/volume) glucose. Sterile plastic microdilution plates containing 96 flat-bottomed wells were utilized. Stock solution of fluconazole was diluted in SC medium and dispensed in $75\,\mu$L volumes into six replicate wells to yield nine two-fold serial dilutions of fluconazole with final concentrations ranging between $0-64\,\mu$g/mL. For each drug concentration, three of the six replicate wells were filled with additional $75\,\mu$L from the *C. albicans* strain suspension while the remaining three wells were filled with $75\,\mu$L from the *C. glabrata* strain suspension. The plate was sealed with a transparent adhesive seal and two holes were punctured over each well by means of a sterile needle. The plate was incubated at 30^oC with shaking over 24 hours and growth monitored by measuring the absorbance of the cell suspensions at 650 nm (A_{650}). Absorbance units were converted into number of cells per ml by means of calibration curves prepared for each *Candida* species.

Drug susceptibility dose-response for *C. albicans* and *C. glabrata*

Standard micro-dilution susceptibility testing was performed in sterile 96-well flat-bottom microtiter plates with the following modifications. Fluconazole was diluted from a 2mg/mL stock solution to a dilution series ranging from 512 to $0\,\mu$g/mL in SC media containing 1% or 4% glucose (weight/volume), at a volume of $75\,\mu$L per well. Overnight cultures in YPD of *C. glabrata* and

C. albicans were counted by haemocytometer and diluted to 10^5 cells/mL in SC broth containing either 1% or 4% glucose. For each species, $75\,\mu L$ of cell suspension was added per well, resulting in a final volume of $150\,\mu L$ which contained 5×10^4 cells, a final drug concentration of $256, 192, 128, 96, 64, 48, 32, 16, 8, 4, 2$ or $0\,\mu g/mL$ of fluconazole and either 1% or 4% glucose. The plate was sealed with a transparent adhesive seal and two holes were punctured over each well, by means of a sterile needle, for aeration. Plates were incubated for 48 hours at 30^oC after which final absorbance was measured at A_{595}. All samples were assayed in technical triplicate.

Competition of *C. albicans* and *C. glabrata* in the absence/presence of drugs

Overnight cultures in YPD of *C. albicans* and *C. glabrata* were diluted, counted on hemocytometer, and adjusted to 2×10^7 cells/mL in SC medium containing either 0.1, 2, or 4% (weight/volume) glucose. The two *Candida* species were then mixed to achieve a range of starting ratios ($0, 10, 30, 50, 70, 90$ and 100% *C. albicans*) The cell suspension was then diluted 1:1 in SC media containing two times desired fluconazole concentration (0, 0.5, or $2\,\mu g/mL$) to a final volume of $150\,\mu L$ in a 96 well flat bottom microtiter plate. Plates were sealed using sterile adhesive films, two holes were punched in seal above each well using a sterile needle, and incubated overnight in orbital shaker set at 30^oC, 180 rpm. Each condition was repeated in triplicate. After 24 hour incubation period (one season) plates were opened, the contents of the well were vigorously pipetted to achieve a homogenous cell suspension, and relative frequency of *C. albicans* ACT1-GFP was determined by flow cytometry in the following way (Supporting Fig. S1). Cellular fluorescence from GFP was determined quantitatively with a FACSAria flow cytometer (Becton Dickinson, CA, USA) equipped with a 20mW, 488 nm argon ion laser. All samples were suspended in phosphate buffered saline (PBS) and briefly sonicated to disperse potential cell clumps prior to analysis. Typically, 10000 cells were analysed per competition sample with the following settings: forward scatter (150 V, log mode) and side scatter (200 V, log mode). GFP was detected on a $530/30$ filter (600 V, log mode) and sample acquisition was performed using BD FACSDiva software. Initially, a sample consisting of *C. albicans* ACT1-GFP cells only was detected and gated to contain $99 - 100\%$ of all measured events as positive for GFP fluorescence. All events occurring within the gate during subsequent analysis of competition samples were considered to be *C. albicans* ACT1-GFP cells. For any given competition sample, the frequency of gated events was calculated by means of FlowJo software and was taken to be the population

percentage of *C. albicans* ACT1-GFP within the sample.

Long-term competition of *C. albicans* and *C. glabrata* for different drug regimes

Overnight cultures in YPD of *C. albicans* and *C. glabrata* were diluted, counted on hemocytometer, and adjusted a 1:1 ratio of each species, at a final concentrations of 2×10^7 cells/mL in SC medium containing either 0.1, or 4% (weight/volume) glucose. The cell suspension was then diluted 1:1 in SC media containing two times desired fluconazole concentration ($3\,\mu g/mL$) and the matching glucose concentration, to a final volume of $150\,\mu L$ in a 96 well flat bottom microtiter plate. Plates were sealed using sterile adhesive films, two holes were punched in seal above each well using a sterile needle, and incubated overnight in orbital shaker set at 30^oC, 180 rpm. Each treatment was repeated in triplicate. After 24 hour incubation period (one season) plates were opened, the contents of the well were vigorously pipetted to achieve a homogenous cell suspension, and five microliters of cell suspension was added to a new well containing $145\,\mu L$ of SC media which contained either the same, or a reduced concentration of glucose and fluconazole. Specifically, for treatment α the cultures were maintained in 0.1% glucose throughout, while the fluconazole concentration was adjusted each season ($3, 2, 1, 0.5,\ 0\,\mu g/mL$). For treatment β the glucose concentration remained at 0.1% and fluconazole concentration at $0.5\,\mu g/mL$ throughout the duration of the experiment. Lastly, for treatment γ both glucose and fluconazole concentrations were reduced each season, glucose decreasing from 4 to 0.1% $(4, 2, 1, 0.5, 0.1)$ and fluconazole decreasing from 3 to $0\,\mu g/mL$ $(3, 2, 1, 0.5, 0)$. Note that $5\mu L$ represents the smallest volume transfer that ensures the accuracy of pipetting is maintained. The relative frequency of *C. albicans* was monitored either by flow cytometry or CFUs, as described above. For daily monitoring $9 - 12$ replicate biological samples were measured, while at the endpoint all replicates were analysed (48 replicates for treatment α, 96 replicates for treatment β and 55 replicates for treatment γ).

Oscillatory (a repeated on-off) drug treatment

Overnight cultures in YPD of *C. albicans* and *C. glabrata* were diluted, counted on hemocytometer, and adjusted a 1:1 ratio of each species, at a final concentrations of 2×10^7 cells/mL in SC medium containing 0.1% (weight/volume) glucose. The cell suspension was then diluted 1:1 in SC media containing two times desired fluconazole concentration (0, 2, or $4\,\mu g/mL$) to a final volume of

$150\,\mu$L in a 96 well flat bottom microtiter plate. Plates were sealed using sterile adhesive films, two holes were punched in seal above each well using a sterile needle, and incubated overnight in orbital shaker set at 30^oC, 180 rpm. Each condition was repeated in triplicate. After 24 hour incubation period (one season) plates were opened, the contents of the well were vigorously pipetted to achieve a homogenous cell suspension, and five microliters of cell suspension was added to a new well containing $145\,\mu$L of SC media which contained the same drug concentration as the day prior, for three days. At day three through day 14, cells were cultured without drug. On day 14 all conditions were treated with $2\,\mu$g/mL fluconazole for an additional three day (through day 17) at which point drug was again omitted from culturing through end of experiment. All wells were passaged daily, on days with data points shown in Figure 1a a volume of suspension was removed for sampling. To monitor relative frequency of each *Candida* species, colony forming units (CFU) were enumerated by plating on YPD agar either with or without the *C. albicans* strain selection nourseothricin (NAT) at $200\,\mu$g/mL. Briefly, cell suspension from overnight culture was diluted to roughly 200 CFU/ $100\,\mu$L and plated on both YPD and YPD+NAT plates, each well was plated in duplicate. Plates were incubated at 30^oC for 48 hours and colonies counted, with the percent *C. albicans* being determined by the ratio of NAT resistant cells to total cells on untreated YPD plates.

Intracellular fluconazole accumulation

The accumulation of fluconazole for both *C. albicans* and *C. glabrata* was analyzed in energized cells in the presence of glucose using the protocol described in (*63*). Cells were incubated with [^{3}H]-FLC (specific activity 740 GBa/mmol, 20 Ci/mmol, 2×10^4 CPM/pmol, $1\,\mu$Ci/ μL; $50\,\mu$M FLC; custom synthesis by Amersham Biosciences, UK). Cells were grown overnight in CSM complete medium at 30°C to a density typically between OD_{600} 6.0 to 8.0, unless otherwise noted. Cells were subsequently harvested by centrifugation ($3000\times$ g, 5 m) and washed three times with YNB complete (1.7 g yeast nitrogen base without amino acids or ammonium sulfate, 5 g ammonium sulfate per liter, pH 5.0) without glucose (for starvation) and without supplementation, unless otherwise noted. Cells were resuspended at an OD_{600} of 75 in YNB for $2-3$h for glucose starvation. Reaction mixes consisted of $250\,\mu$L of YNB, $200\,\mu$L of cells (75 OD) and $50\,\mu$L of [^{3}H]-FLC ($1/100$ dilution of stock). The resulting [^{3}H]-FLC concentration is 50 nM ($0.015\,\mu$g/mL), which is significantly below the MIC for all strains. Samples ($100\,\mu$L) were removed at various time points and placed into 5 ml stop solution

(YNB $+20$ mM [$6\,\mu g/mL$] FLC), filtered on glass fibre filters (24 mm GF/C; Whatman; Kent, UK) pre-wetted with stop solution and washed with 5 ml of stop solution. Filters were transferred to 20 ml scintillation vials. Scintillation cocktail (Ecoscint XR, National Diagnostics, Atlanta GA) was added (15 ml) and the radioactivity associated with the filter was measured with a liquid scintillation analyzer (Tri-Carb 2800 TR; Perkin Elmer; Waltham, MA) and normalized to CPM$/1 \times 10^8$ cells. Rate of [^{3}H]-FLC uptake was determined by incubating samples in the presence of increasing concentrations of unlabeled FLC (unless otherwise noted) and samples were analyzed for [^{3}H]-FLC accumulation at designated time points.

Computational methods

Numerical simulations of a theoretical community model were obtained using Matlab's differential equation solvers to generate the season-by-season dynamical map $\Phi(f)$. Differential equations were parameterised using data from *C. albicans* and *C. glabrata*, as detailed in the supplementary.

To determine tipping points, we sought significant increases in between-replicated variation (BRV) defined as follows. If $\mathcal{F} = \{f_j\}_{j=1}^n$ is the set of observed *C. albicans* frequencies, expressed as values between zero and one (although some figures express this as a percentage), the set of between-replicate differences is then $\{|f_j - f_k|\}_{j,k=1,j>k}^n$ and mean BRV is the mean of this set; note, this is one form of set radius. As the frequency of *C. glabrata* is $G_j = 1-f_j$ and $G_j - G_k = 1-f_j-(1-f_k) = f_k - f_j$, *C. glabrata* frequency data has the same between-replicate differences as *C.albicans*.

Kernel density estimates were obtained for distributions of BRV values (Figure 4(a)) using a kernel estimation algorithm implemented in Matlab (*64*). To test for significant season-by-season differences in BRV, BRV$_n$ and BRV$_{n+1}$ observed at seasons n and $n+1$, we applied linear regression to test (with $p < 0.001$) against the null hypothesis of a constant mean BRV between those seasons, testing for a non-zero slope parameter from the regression. This is written ΔBRV and this change was found to be largest for season 6 of treatment γ (Figure 4(b)).

Reporting Summary

Further information on experimental design is available in the Nature Research Reporting Summary linked to this article.

Data availability statement

All experimental data generated during this study can be found at https://doi.org/10.24378/exe.345.

References and Notes

1. Payne, D. J., Gwynn, M. N., Holmes, D. J. & Pompliano, D. L. Drugs for bad bugs: confronting the challenges of antibacterial discovery. *Nat Rev Drug Discov* **6**, 29–40 (2007).

2. Mira, P. M. *et al.* Rational design of antibiotic treatment plans: A treatment strategy for managing evolution and reversing resistance. *PLoS ONE* **10**, 1–25 (2015).

3. Kollef, M. H. Is antibiotic cycling the answer to preventing the emergence of bacterial resistance in the intensive care unit? *Clin.Infect.Dis.* **43 Suppl 2**, S82–S88 (2006).

4. Sundqvist, M. Reversibility of antibiotic resistance. *Upsala journal of medical sciences* **119**, 142–8 (2014).

5. Lee, J. *et al.* Control of extended-spectrum beta-lactamase-producing Escherichia coli and Klebsiella pneumoniae in a children's hospital by changing antimicrobial agent usage policy. *Journal of Antimicrobial Chemotherapy* **60**, 629–637 (2007).

6. Rahal, J. J. *et al.* Class restriction of cephalosporin use to control total cephalosporin resistance in nosocomial Klebsiella. *Jama* **280**, 1233–1237 (1998).

7. Cook, P. P., Catrou, P. G., Christie, J. D., Young, P. D. & Polk, R. E. Reduction in broad-spectrum antimicrobial use associated with no improvement in hospital antibiogram. *Journal of Antimicrobial Chemotherapy* **53**, 853–859 (2004).

8. Nijssen, S. *et al.* Effects of reducing beta-lactam antibiotic pressure on intestinal colonization of antibiotic-resistant gram-negative bacteria. *Intensive Care Medicine* **36**, 512–519 (2010).

9. Chong, Y. *et al.* Antibiotic Rotation for Febrile Neutropenic Patients with Hematological Malignancies: Clinical Significance of Antibiotic Heterogeneity. *PLoS ONE* **8** (2013).

10. Takesue, Y. *et al.* Impact of a hospital-wide programme of heterogeneous antibiotic use on the development of antibiotic-resistant Gram-negative bacteria. *Journal of Hospital Infection* **75**, 28–32 (2010).

11. Hashino, S. *et al.* Clinical impact of cycling the administration of antibiotics for febrile neutropenia in Japanese patients with hematological malignancy. *European Journal of Clinical Microbiology and Infectious Diseases* **31**, 173–178 (2012).

12. Sarraf-Yazdi, S. *et al.* A 9-year retrospective review of antibiotic cycling in a surgical intensive care unit. *Journal of Surgical Research* **176**, e73–e78 (2012).

13. Gruson, Didier; Gilles, Hilbert; Vargas, F. Rotation and Restricted Use of Antibiotics in a Medical Intensive Care Unit. *American Journal of Respiratory and Critical Care Medicine* **162**, 837–843 (2000).

14. Van Loon, H. J. *et al.* Antibiotic rotation and development of Gram-negative antibiotic resistance. *American Journal of Respiratory and Critical Care Medicine* **171**, 480–487 (2004).

15. Warren, D. *et al.* Cycling empirical antimicrobial agents to prevent emergence of antimicrobial-resistant Gram-negative bacteria among intensive care unit patients. *Crit Care Med* **32**, 2450–6 (2004).

16. Andersson, D. I. & Hughes, D. Antibiotic resistance and its cost: is it possible to reverse resistance? *Nat Rev Microbiol* **8**, 260–271 (2010).

17. Gonze, D., Lahti, L., Raes, J. & Faust, K. Multi-stability and the origin of microbial community types. *ISME J* **11**, 2159–2166 (2017).

18. Panda, S. *et al.* Short-term effect of antibiotics on human gut microbiota. *PLoS ONE* **9** (2014).

19. Jakobsson, H. E. *et al.* Short-term antibiotic treatment has differing long- term impacts on the human throat and gut microbiome. *PLoS ONE* **5** (2010).

20. Dethlefsen, L., McFall-Ngai, M. & Relman, D. a. An ecological and evolutionary perspective on human-microbe mutualism and disease. *Nature* **449**, 811–8 (2007).

21. Antonopoulos, D. A. *et al.* Reproducible community dynamics of the gastrointestinal microbiota following antibiotic perturbation. *Infection and Immunity* **77**, 2367–2375 (2009).

22. Perez-Cobas, A. E. *et al.* Gut microbiota disturbance during antibiotic therapy: a multi-omic approach. *Gut* **62**, 1591–1601 (2013).

23. Dethlefsen, L. & Relman, D. A. Incomplete recovery and individualized responses of the human distal gut microbiota to repeated antibiotic perturbation. *Proc Natl Acad Sci U S A* **108 Suppl**, 4554–4561 (2011).

24. McFarland, L. V., Elmer, G. W. & Surawicz, C. M. Breaking the cycle: treatment strategies for 163 cases of recurrent clostridium difficile disease. *Am J Gastroenterol* **97**, 1769–1775 (2002).

25. Cousin, L., Berre, M. L., Launay-Vacher, V., Izzedine, H. & Deray, G. Dosing guidelines for fluconazole in patients with renal failure. *Nephrol Dial Transplant* **18**, 2227–2231 (2003).

26. Ashbee, H. R. *et al.* Therapeutic drug monitoring (tdm) of antifungal agents: guidelines from the british society for medical mycology. *J Antimicrob Chemother* **69**, 1162–1176 (2014).

27. Havey, T. C., Fowler, R. A., Pinto, R., Elligsen, M. & Daneman, N. Duration of antibiotic therapy for critically ill patients with bloodstream infections: A retrospective cohort study. *Can J Infect Dis Med Microbiol* **24**, 129–137 (2013).

28. Cowart, S. L. & Stachura, M. E. *Glucosuria* (Butterworth Publishers, a division of Reed Publishing, 1990).

29. Carlotti, A. P. C. P. *et al.* A hyperglycaemic hyperosmolar state in a young child: diagnostic insights from a quantitative analysis. *QJM* **100**, 125–137 (2007).

30. Manoj, G., George, M. R., Dipu, R. & Jishnu, J. The survival story of a diabetic ketoacidosis patient with blood sugar levels of 1985 mg/dl **8**, 60–61 (2017).

31. m. Ho, K. & s. Cheng, T. Common superficial fungal infections, a short review. *Medical Bulletin* **15**, 23–27 (2010).

32. Wenzel, R. P. & Gennings, C. Bloodstream infections due to Candida species in the intensive care unit: identifying especially high-risk patients to determine prevention strategies. *Clinical Infectious Diseases* **41 Suppl 6**, S389–93 (2005).

33. Brown, G. D. *et al.* Hidden killers: human fungal infections. *Sci Transl Med* **4**, 165rv13 (2012).

34. Kett, D. H., Azoulay, E., Echeverria, P. M. & Vincent, J.-L. Candida bloodstream infections in intensive care units: analysis of the extended prevalence of infection in intensive care unit study. *Crit Care Med* **39**, 665–670 (2011).

35. Pappas, P. G. *et al.* Guidelines for treatment of candidiasis. *Clinical infectious diseases : an official publication of the Infectious Diseases Society of America* **38**, 161–89 (2004).

36. Rex, J. H. *et al.* Development of interpretive breakpoints for antifungal susceptibility testing: conceptual framework and analysis of in vitro-in vivo correlation data for fluconazole, itraconazole, and candida infections. subcommittee on antifungal susceptibility testing of the national committee for clinical laboratory standards. *Clin Infect Dis* **24**, 235–247 (1997).

37. Lortholary, O. *et al.* Recent exposure to caspofungin or fluconazole influences the epidemiology of candidemia: a prospective multicenter study involving 2,441 patients. *Antimicrob Agents Chemother* **55**, 532–538 (2011).

38. Hibbing, M. E., Fuqua, C., Parsek, M. R. & Peterson, S. B. Bacterial competition: surviving and thriving in the microbial jungle. *Nat Rev Microbiol* **8**, 15–25 (2010).

39. Scheffer, M., Carpenter, S., Foley, J. a., Folke, C. & Walker, B. Catastrophic shifts in ecosystems. *Nature* **413**, 591–6 (2001). URL `http://www.ncbi.nlm.nih.gov/pubmed/15448261`.

40. Lenton, T. M. *et al.* Tipping elements in the Earth's climate system. *Proceedings of the National Academy of Sciences* **105**, 1786–1793 (2008).

41. Wissel, C. A universal law of the characteristic return time near thresholds. *Oecologia* **65**, 101–107 (1984).

42. Wiesenfeld, K. & Mcnamara, B. Small-signal amplification in bifurcating dynamical systems. *Physical Review A* **33**, 629–642 (1986).

43. Dai, L., Vorselen, D., Korolev, K. S. & Gore, J. Generic Indicators for Loss of Resilience Before a Tipping Point Leading to Population Collapse. *Science* **336**, 1175–1177 (2012).

44. Scheffer, M. *et al.* Early-warning signals for critical transitions. *Nature* **461**, 53–59 (2009).

45. Dakos, V. *et al.* Slowing down as an early warning signal for abrupt climate change. *Proceedings of the National Academy of Sciences of the United States of America* **105**, 14308–12 (2008). arXiv:1408.1149.

46. Lenton, T. M. Early warning of climate tipping points. *Nature Climate Change* **1**, 201–209 (2011). URL http://dx.doi.org/10.1038/nclimate1143.

47. Carpenter, S. R. & Brock, W. A. Rising variance: A leading indicator of ecological transition. *Ecology Letters* **9**, 308–315 (2006). 1107.3639.

48. Guttal, V. & Jayaprakash, C. Changing skewness: An early warning signal of regime shifts in ecosystems. *Ecology Letters* **11**, 450–460 (2008).

49. Baillie, G. S. & Douglas, L. J. Effect of growth rate on resistance of candida albicans biofilms to antifungal agents. *Antimicrob Agents Chemother* **42**, 1900–1905 (1998).

50. Basson, N. J. Competition for glucose between candida albicans and oral bacteria grown in mixed culture in a chemostat. *J Med Microbiol* **49**, 969–975 (2000).

51. Huang, M., McClellan, M., Berman, J. & Kao, K. C. Evolutionary dynamics of candida albicans during in vitro evolution. *Eukaryot Cell* **10**, 1413–1421 (2011).

52. Ene, I. V., Brunke, S., Brown, A. J. P. & Hube, B. Metabolism in fungal pathogenesis. *Cold Spring Harb Perspect Med* **4**, a019695 (2014).

53. MacLean, R. C. & Gudelj, I. Resource competition and social conflict in experimental populations of yeast. *Nature* **441**, 498–501 (2006).

54. Fidel Jr., P. L., Vazquez, J. A. & Sobel, J. D. Candida glabrata: review of epidemiology, pathogenesis, and clinical disease with comparison to C. albicans. *Clinical Microbiology Reviews* **12**, 80–96 (1999).

55. Ray, D. *et al.* Prevalence of Candida glabrata and its response to boric acid vaginal suppositories in comparison with oral fluconazole in patients with diabetes and vulvovaginal candidiasis. *Diabetes Care* **30**, 312–317 (2007).

56. Sonnenburg, E. D. *et al.* Specificity of polysaccharide use in intestinal bacteroides species determines diet-induced microbiota alterations. *Cell* **141**, 1241–1252 (2010). NIHMS150003.

57. David, L. A. *et al.* Diet rapidly and reproducibly alters the human gut microbiome. *Nature* **505**, 559–63 (2014). NIHMS150003.

58. Metzler-Zebeli, B. U., Lange, J. C., Zijlstra, R. T. & Gänzle, M. G. Dietary non-starch polysaccharides alter the abundance of pathogenic clostridia in pigs. *Livestock Science* **152**, 31–35 (2013).

59. Allison, K. R., Brynildsen, M. P. & Collins, J. J. Metabolite-enabled eradication of bacterial persisters by aminoglycosides. *Nature* **473**, 216–220 (2011).

60. Peng, B. *et al.* Exogenous alanine and/or glucose plus kanamycin kills antibiotic-resistant bacteria. *Cell Metab* **21**, 249–261 (2015).

61. Zampieri, M. *et al.* Metabolic constraints on the evolution of antibiotic resistance. *Molecular Systems Biology* **13**, 917 (2017).

62. Milne, S. W., Cheetham, J., Lloyd, D., Aves, S. & Bates, S. Cassettes for PCR-mediated gene tagging in Candida albicans utilizing nourseothricin resistance. *Yeast* **3**, 833–841 (2011).

63. Mansfield, B. E. *et al.* Azole Drugs Are Imported By Facilitated Diffusion in Candida albicans and Other Pathogenic Fungi. *PLoS Pathogens* **6**, 11 (2010).

64. Botev, Z. I., Grotowski, J. F. & Kroese, D. P. Kernel density estimation via diffusion. *Ann. Statist.* **38**, 2916–2957 (2010).

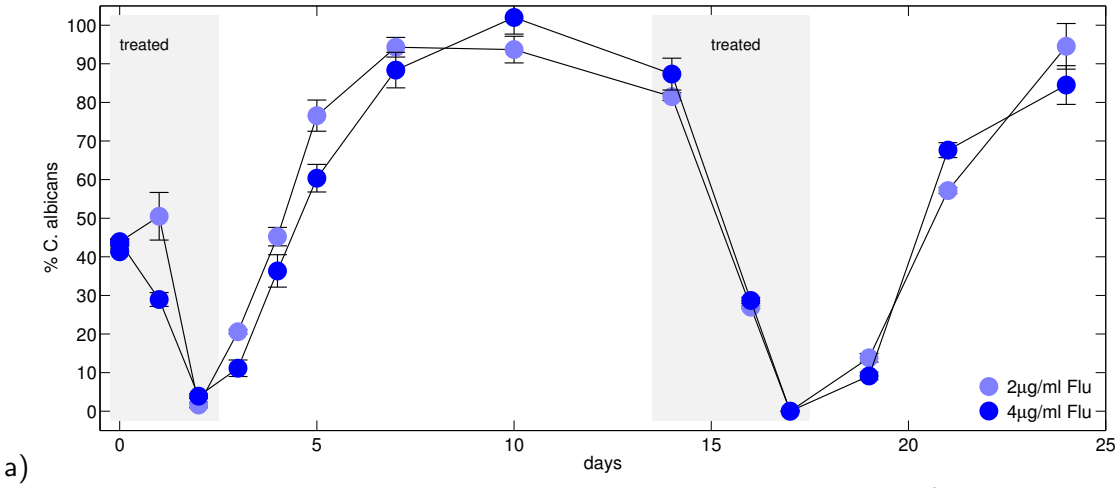
a)
treated
treated
% C. albicans
days
2µg/ml Flu
4µg/ml Flu

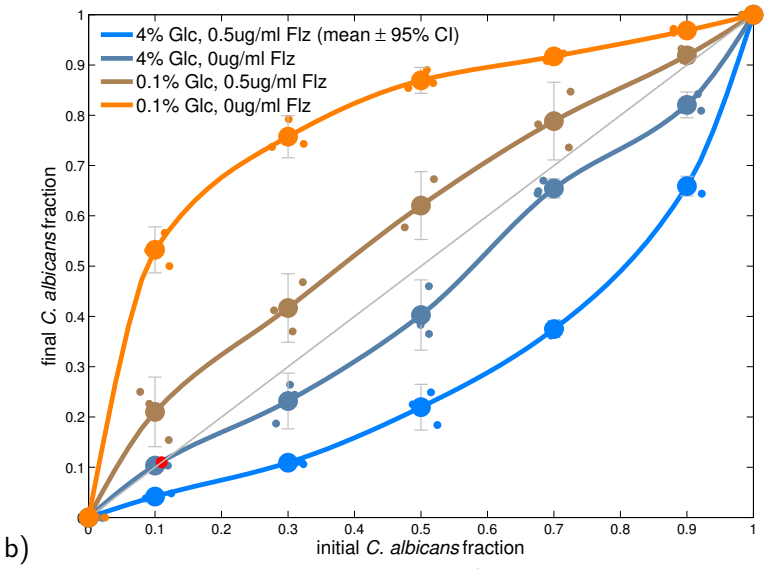
b)
4% Glc, 0.5ug/ml Flz (mean ± 95% CI)
4% Glc, 0ug/ml Flz
0.1% Glc, 0.5ug/ml Flz
0.1% Glc, 0ug/ml Flz
final C. albicans fraction
initial C. albicans fraction

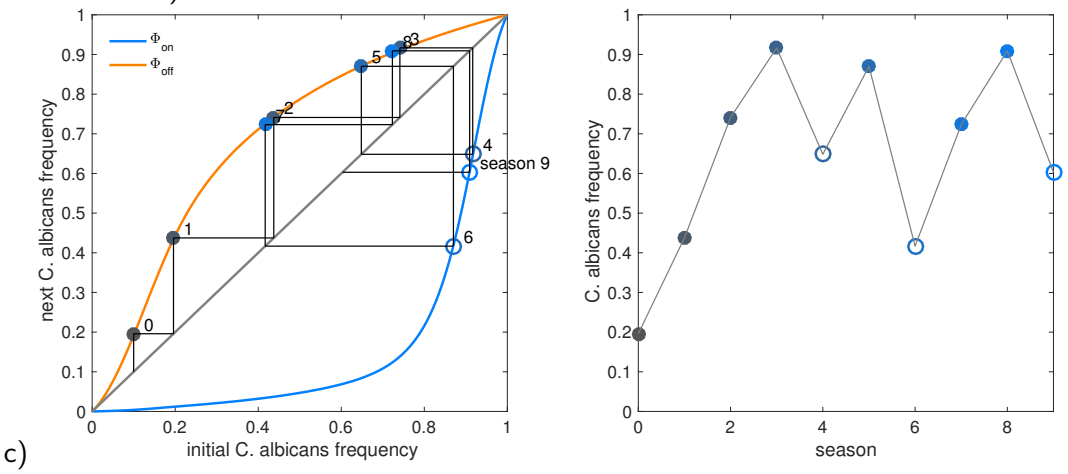
c)
Φon
Φoff
next C. albicans frequency
initial C. albicans frequency
season 9
C. albicans frequency
season

Figure 1: a) Lab data: *C. albicans* and *C. glabrata* are inoculated at 50-50 proportions into growth in SC media supplemented with 0.1% glucose and propagated in the presence of fluconazole for 2 seasons, the *C. albicans* frequency subsequently decreases. After 2 seasons, fluconazole is withdrawn and *C. albicans* recovers. When fluconazole is later re-applied for 3 seasons *C. albicans* again decreases in frequency, and so the cycle repeats. (Grey boxes mark seasons undergoing fluconazole treatment, error bars are mean $\pm$ 95% CI, $n = 3$, raw data shown.) b) Lab data: the initial *C. albicans* frequency (f) on the x-axis versus the final frequency each season obtained using the laboratory microcosm on the y-axis, aka $\Phi(f)$ (four exemplars are shown; error bars are mean $\pm$ 95% CI, $n = 3$; glucose and fluconazole given in the legend, SC denotes synthetic complete media). c) Theoretical example: how to read $\Phi(f)$ to understand dynamics: starting at timepoint 0, the dynamics follow Φ_{on} while treatment proceeds, it then follows Φ_{off} when treatment stops. The sequence of treatments here is (on,on,on,on,off,on,off,on,on,off). The right plot shows how *C. albicans* reversibly increases and decreases in frequency according to whether drug is used (solid dot) or not (open circle).

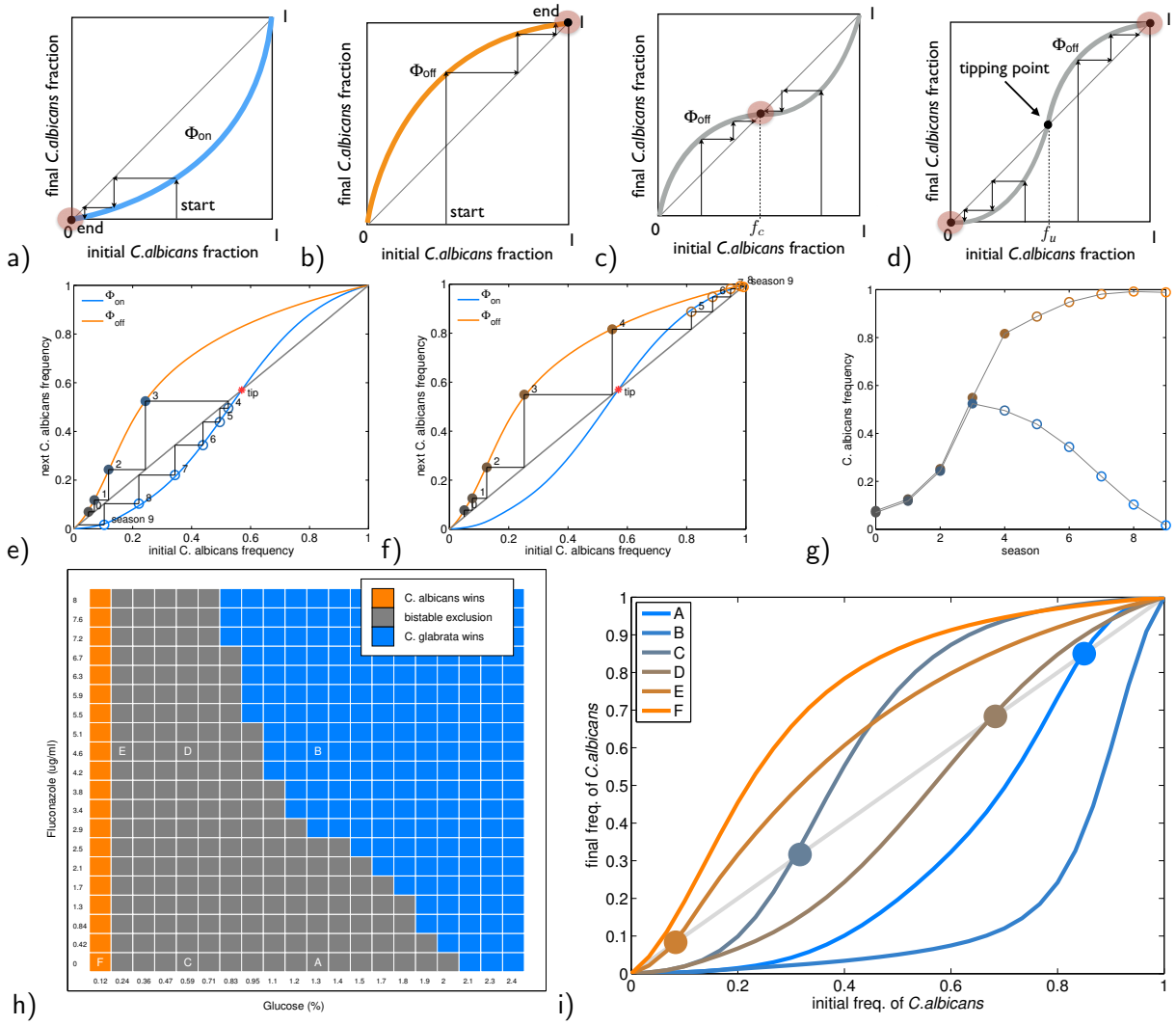
a)
final C.albicans fraction
initial C.albicans fraction
Φon
start
end
b)
Φoff
start
end
c)
Φoff
$\hat{f}_c$
d)
Φoff
tipping point
$\hat{f}_u$
e)
Φon
Φoff
next C. albicans frequency
initial C. albicans frequency
tip
season 9
f)
season 9
g)
C. albicans frequency
season
h)
C. albicans wins
bistable exclusion
C. glabrata wins
Fluconazole (μg/ml)
Glucose (%)
i)
A
B
C
D
E
F
final freq. of C.albicans
initial freq. of C.albicans

Figure 2: Population dynamics theory states that one can deduce multi-season frequency dynamics from the 'cobweb diagram' determined from the initial *C. albicans* frequency plotted versus the final frequency each season. a): $\Phi_{\rm on}$ lies below the diagonal so *C. glabrata* outcompetes *C. albicans*. b) $\Phi_{\rm off}$ lies above the diagonal line of equal frequencies, so *C. albicans* outcompetes *C. glabrata*. c) $\Phi_{\rm off}$ is such that there exist a special frequency, f_c, which lies on the diagonal line and $\Phi_{\rm off}(f) > f$ for $0 < f < f_c$ while $\Phi_{\rm off}(f) < f$ for $f_c < f < 1$, this is a stable coexistence state. d) $\Phi_{\rm off}$ is such that there exist a special frequency, f_u, which lies on the diagonal line and $\Phi_{\rm off}(f) < f$ for $0 < f < f_u$ while $\Phi_{\rm off}(f) > f$ for $f_u < f < 1$. In this case either species can dominate depending on their initial frequencies: if the initial frequency of *C. albicans* is smaller than f_u then *C. albicans* loses out in competition to *C. glabrata*, otherwise *C. glabrata* loses out; this is 'bistable exclusion'. e) A theoretical example of a 3-season treatment, which stops short of the tipping point (marked 'tip') with seasons 4-9 continuing without the drug being applied. f) A theoretical example of a 4-season treatment which goes beyond the tipping point, causing the divergence in trajectories following drug withdrawal cause by the tipping point as shown in (g). h) This is a theoretical two-dimensional *dose-response mosaic*, it describes the equilibrium outcome of competition in the *Candida* community as glucose and fluconazole are varied. *C. albicans* wins the competition inside orange squares, *C. glabrata* wins inside the blue squares and bistable exclusion occurs in the grey squares. Drug on-off treatments that encounter the latter may exhibit tipping (e.g. ABAB, FEFE and CDCD treatment sequences), treatments that stay inside the former will exhibit reversible resistance (e.g. an FBFB sequence). i) theoretical Φ functions at points A-F in the dose response mosaic, with dots highlighting the location of the special frequency f_u for each Φ that crosses the diagonal.

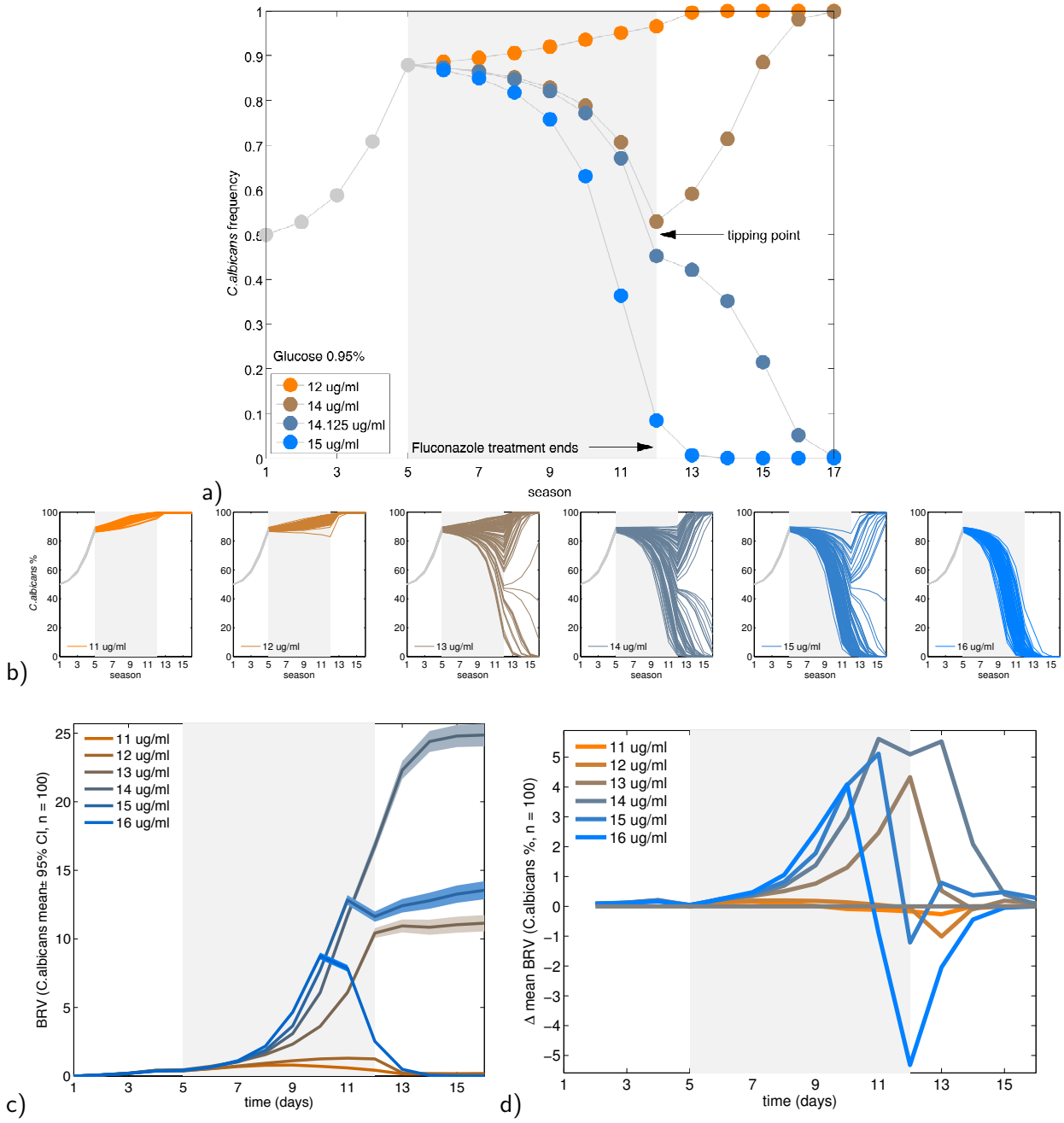
a)
C.albicans frequency
season
Glucose 0.95%
12 ug/ml
14 ug/ml
14.125 ug/ml
15 ug/ml
tipping point
Fluconazole treatment ends
b)
C.albicans %
11 ug/ml
12 ug/ml
13 ug/ml
14 ug/ml
15 ug/ml
16 ug/ml
c)
BRV (C.albicans mean± 95% CI, n = 100)
time (days)
d)
Δ mean BRV (C.albicans %, n = 100)
time (days)

Figure 3: The dose-response mosaic shows tipping points are encountered in many ways, for example by varying glucose concentration (see Supporting Fig. S10 for details) or as fluconazole concentration is varied (a). In (a) four, fixed-dose treatments start on season 5 and end on season 12 (grey box) at a 0.95% (by volume) glucose dose. First, the community converges towards *C. albicans* domination in the absence of drug (orange dots). *C. glabrata* starts to dominate as drug is applied, but it rescinds when treatment ends (brown dots) and the community returns to its pre-treatment composition and then continues towards *C. albicans* dominance with more seasons. However, a tipping point appears at just high-enough fluconazole dose (dark blue dots) whereby the post-treatment trajectory diverges from the previous outcome (at a slightly lower drug dose) and *C. albicans* is lost as the seasons pass. Royal blue dots show trajectories at dosages well above the tipping point. (b) Introducing additive stochastic noise to simulations from (a) shows that replicate trajectories diverge at the tipping point, creating large variations between frequency trajectories that had identical drug dosage regimes and initial *Candida* frequencies. A signature we can seek in empirical data: between replicate variation (BRV) spikes at the tipping point (c), causing a large season-by-season change in BRV (ΔBRV here taken to be the mean change in standard deviation) that is significantly positive at the tipping point (d).

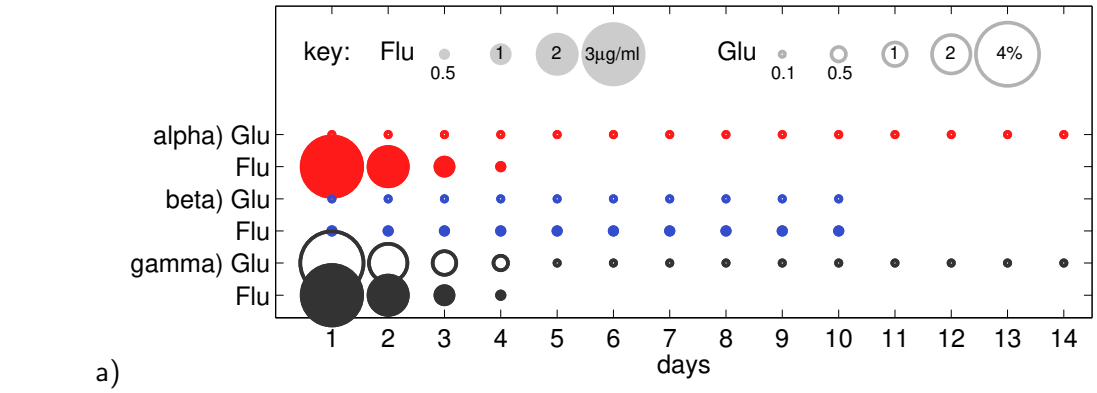
key: Flu 0.5 1 2 3µg/ml Glu 0.1 0.5 1 2 4%
alpha) Glu
Flu
beta) Glu
Flu
gamma) Glu
Flu
1 2 3 4 5 6 7 8 9 10 11 12 13 14
days

a)

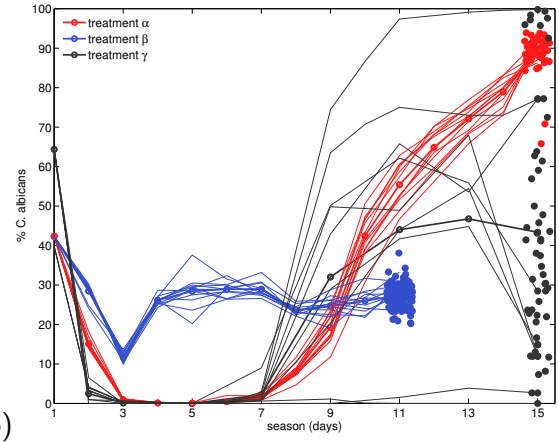
treatment α
treatment β
treatment γ
% C. albicans
season (days)

b)

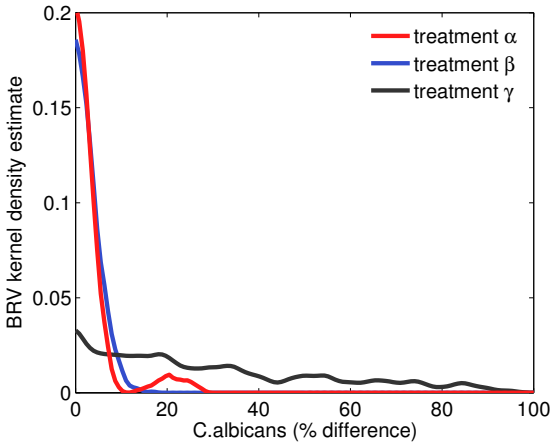
treatment α
treatment β
treatment γ
BRV kernel density estimate
C.albicans (% difference)

c)

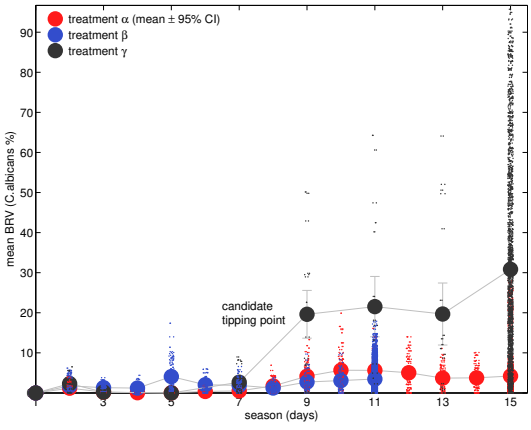
treatment α (mean ± 95% CI)
treatment β
treatment γ
mean BRV (C.albicans %)
candidate tipping point
season (days)

d)

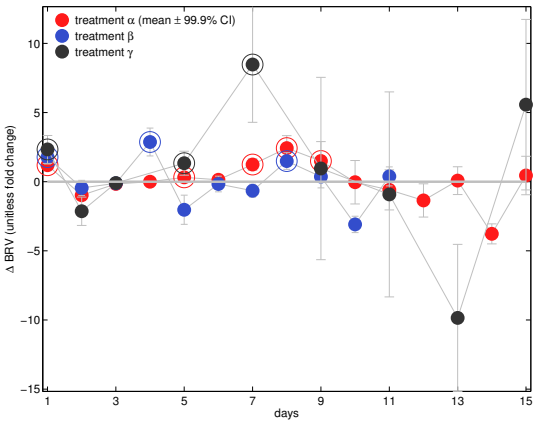
treatment α (mean ± 99.9% CI)
treatment β
treatment γ
Δ BRV (unitless fold change)
days

e)

Figure 4: a) Three laboratory treatments with different dynamics: treatments α (red) and γ (black) withdraw fluconazole but β (blue) keeps it at constant levels (dosages represented as circle sizes). The laboratory experimental trajectories of treatments are shown in (b) and the corresponding between-replicate variation (BRV) is shown in (c) as indicated by the kernel density estimate of the distribution of final-season *C. albicans* frequency differences (48 replicates for α, 96 for β and 55 for γ). The trajectories of treatments α and β have low BRV in species frequencies at all times whereas γ has high BRV at the end of treatment. The trajectories show why: community dynamics for β maintain steady-state and *C.albicans* sweeps through the community during treatment α following drug withdrawal. However, in γ trajectories of different replicates vary markedly beyond season 6 whereby either species can dominate by season 14, despite all replicates having close to 50-50 initial composition (Supporting Fig. S11 has additional data). d) Data from the *Candida* community shows mean BRV increases significantly, approximately 8-fold for treatment γ on season 6. Treatments α and β also have significant increases on occasion, but by no more than 3-fold. Taking a conservative Bonferroni-corrected significance at the level $p < 0.001$ in an F-test using linear regression (see Methods), significant changes in mean BRV are shown in (e) as circled dots. The largest increase (approximately 8-fold) is significant and occurs in treatment γ on season 7 (error bars explained in legend).

Acknowledgements

In memory of our friend and colleague Ken Haynes who sadly passed away on 19th March 2018.

Author Contributions

IG and REB conceived the idea; REB, IG and EC designed all experiments (apart from Supporting Fig. S5); TCW designed the experiment in Supporting Fig. S5; EC, SN, ARS, AT, BDE, KH, NARG and AJPB carried out experiments; IG and REB developed and numerically simulated the mathematical model; REB, IG, EC, TCW, KH, NARG and AJPB discussed the results; REB, EC and IG wrote the manuscript.

Competing interests

The authors declare no competing interests